Preliminary Model for Methotrexate Pharmacokinetics

K. B. BISCHOFF*, R. L. DEDRICK, and D. S. ZAHARKO

Abstract □ A pharmacokinetic model is presented to describe the distribution of methotrexate in mice, and the required physicochemical, anatomical, and physiological data are discussed. The model is used to simulate methotrexate concentrations in plasma, lean tissue, liver, kidneys, and gastrointestinal tract following a single intravenous injection. Methotrexate is excreted in the urine and bile; partial reabsorption occurs in the gastrointestinal tract. Tissue-to-plasma distribution ratios were: muscle (0.15:1); kidney (3:1); liver (10:1). Observed bile concentrations were 300 times those of plasma.

Keyphrases □ Methotrexate pharmacokinetics—model □ Distribution, methotrexate—mice □ Tissue/plasma ratios—methotrexate □ Plasma protein binding—methotrexate □ Pharmacokinetic equations—methotrexate absorption, distribution, excretion □ Model, methotrexate distribution—one, two compartments plus gut lumen

This paper presents the results of some first attempts to formulate mathematical models for the distribution of the cancer chemotherapeutic agent methotrexate (MTX) in mammals. It begins with a short discussion of why and how such pharmacokinetic models can be of practical use as well as enhancing insight and appreciation of relevant physiological phenomena.

One important application of the models can be to aid in the evaluation of screening tests. Most cancer chemotherapeutic agents (as well as many other drugs) are initially screened by a series of experimental evaluations using mice. Normally, only the gross success or failure of the drug to combat tumors is considered. The actual sequence of events, however, can be divided into two major aspects: first, the spatial and temporal physical distribution of the drug within the body and, second, the physiological (therapeutic and toxic) effects at discrete tissue loci. The latter, of course, is the crucial issue, but until local concentrations for known time intervals throughout the body are defined, reliable correlations between drug distribution and drug effect cannot be established. Thus the distribution information is required to more fully appreciate the problems of drug evaluation.

If initial screening tests are successful, trials in other animal species, eventually leading to man, are performed. Many relevant interspecies differences are associated with chemical phenomena—such as metabolism, binding, and membrane transport. Physical aspects, such as organ sizes and intracorporeal fluid flow rates, also vary among species. These facts suggest a scale-up approach based on maximum use of physiological, anatomical, and physicochemical information. A reliable quantitative model based on physiology can serve as a useful framework for designing experiments and evaluating results.

Such a model with appropriate scale-up information may significantly enhance success in the ultimate application in the clinic. Concentration history may be predictable at any site as a function of dose schedule and route of administration. This information, coupled with knowledge of drug concentration and exposure time necessary for maximum tumor toxicity, should provide a rational basis for optimization of dosage regimens. This can be critical for cancer chemotherapeutic agents because of the rather narrow range between effective and toxic doses.

RATIONALE AND GENERAL FEATURES OF MODELS

Before discussing the details of the experiments and models for MTX, a few brief statements will be made concerning pharmacokinetic models. The approach used here has been extensively discussed and illustrated elsewhere: Bischoff and Brown (1), Bischoff (2), Dedrick and Bischoff (3), and Bischoff and Dedrick (4). Mass transfer models are based on "lumping" body regions, with similar physicochemical properties, into discrete compartments. Volumes, flows, and other properties will all have independently verifiable anatomical significance. The use of parameters obtained from experiments other than the one being modeled is important, since it can lead to generally applicable *a priori* predictions. Further, the model leads to insight concerning some of the physiological mechanisms.

One broad assumption used in developing the model, that of flow-limited conditions, deserves mention here. This assumption, commonly used in pharmacokinetics, implies that the blood leaving a tissue is in diffusion equilibrium with the tissue, *i.e.*, the free (not protein bound) concentrations of blood and tissue are the same. This assumption requires that membrane permeability is sufficiently larger than the perfusion rate so that the latter is rate controlling. A mathematical criterion for this was given by Dedrick and Bischoff (3) and it was shown that the assumption was valid for certain barbiturates. MTX is not particularly lipid soluble and has a molecular weight of 454; thus, its permeability is probably somewhat lower than the barbiturates. Since there seem to be no numerical values available, the work will be done with flow-limited models, bearing in mind, however, that modifications may be necessary to account for finite permeabilities.

EXPERIMENTAL INVESTIGATIONS

The data discussed here are preliminary in nature from the first of a series of experiments. Only one dose level, 3 mg./kg., is considered. This dose is in the range of clinical therapeutic values [Henderson, Adamson, Denham, and Oliverio (5, 6)]. Other levels will be used in future work. Figure 1 shows the data points from several experiments. The points at any one time represent the distribution of methotrexate (MTX), 3′,5′-tritium labeled in one mouse (CDF-1 male) which is injected i.v. and then sacrificed for tritium analysis of the various tissues. Thus these data represent many mice, which would tend to add variability.

Several features of Fig. 1 will be briefly described as an aid in developing models. The implied curves contain certain typical

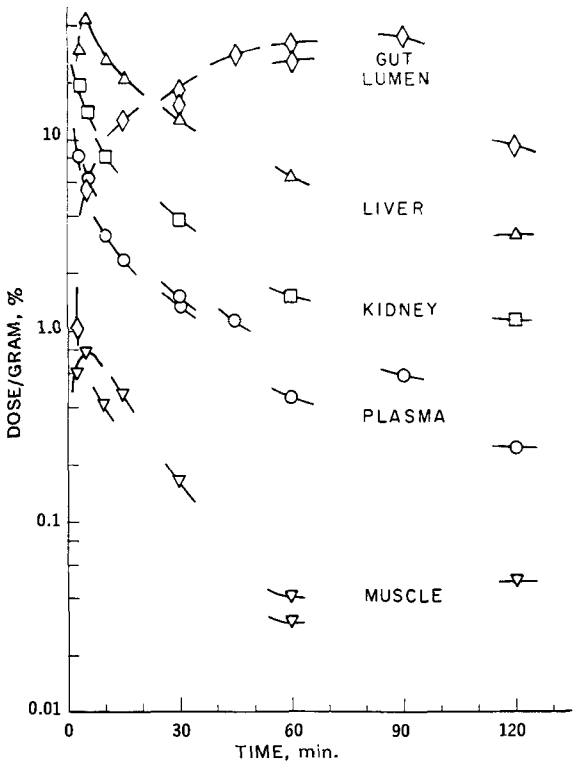

Figure 1—*Distribution of MTX in mice following pulse injection in tail vein.*

features, *e.g.*, immediately following injection there is a short time period of rapid drop in plasma concentration followed by a period of slower rate of decrease. One difference from many drugs, however, is the magnitude of the initial drop. Since Henderson *et al.* (5, 6) have shown that MTX is not appreciably metabolized in mice, this concentration drop results from rapid localization in tissues and excretion. The data points for the small intestine rapidly increase at the outset, which indicates the significant role of the biliary route, as has also been indicated by Henderson *et al.* (5, 6). In fact, 1–2 hr. postinjection, the gut concentration is about 100 times the plasma concentration. From chemical analysis in addition to the radioactivity counting, it appears that the MTX is not conjugated or metabolized in the enterohepatic cycling (5) in contrast to most drugs. The liver here acts differently than with many drugs in that even with its high perfusion rate, several minutes are required to attain maximum concentration. This effect is probably also influenced by biliary clearance and bile formation in the liver.

After a sufficient length of time, all of the curves level asymptotically, suggesting (but not proving) a zero-order absorption from the gut. The tissue/plasma ratios also vary substantially: muscle/plasma ~0.15:1; liver/plasma ~10:1, kidney/plasma ~3:1. These are some of the major characteristics that a successful model must predict.

An essential step in the synthesis of meaningful models is the definition of reliable physical parameters. One obvious set includes the organ weights and flows. The former were obtained from the previously described experiments. The relevant flows are more difficult to obtain, but the model developed here does not require an extensive set. Renal clearance was obtained by comparing integrated plasma concentration data with cumulative urinary excretion. The value was found to be somewhat less than an estimate of inulin clearance based on the literature (7). Little is known about quantitative biliary clearances. These were estimated by separate experiments with anesthetized mice in which the bile duct was cannulated and the flow rate and concentrations directly measured. An estimate of the time delay between injection and appearance of MTX in the bile was also noted.

The data in Fig. 1, together with results published by Henderson *et al.* (5, 6), indicate that gut absorption of MTX may be a zero-order process, in some concentration ranges, presumably caused by saturation of a transport mechanism. The saturation point in humans seems to lie between doses of 0.1–1.0 mg./kg., which is less than our experimental level. An experiment was performed where a known amount of MTX was injected directly into the duodenum and determinations made of the fraction remaining after specific time intervals. Much more experimental work will be required to describe the gut absorption adequately. For the present, zero-order kinetics will be used. Finally, the binding of MTX was evaluated. Plasma protein binding was about 25% and could be correlated with a linear isotherm. Tissue binding is much more difficult to obtain. Separate steady infusion experiments were performed, and the results for the muscle/plasma distribution ratio agreed with that obtained during the kinetic study.

Such separate experiments serve independently to determine or verify most of the model parameters so that generalized *a priori* predictions can be attempted.

MODEL EQUATIONS

Based on the above considerations, the general equations as presented in Dedrick and Bischoff (3) can be considerably simplified. The muscle compartment will be considered to illustrate details. Equations for other compartments are derived similarly. The mass balance accounting for both free and bound drug is:

$$(f_B V_{MB} + f_{MT} V_{MT}) \frac{dC_M}{dt} + (1 - f_B) V_{MB} \frac{dx_{MB}}{dt} + (1 - f_{MT}) V_{MT} \frac{dx_{MT}}{dt} = Q_M[f_B C_P + (1 - f_B) x_B] - Q_M[f_B C_M + (1 - f_B) x_{MB}] \quad \text{(Eq. 1)}$$

where the terms are defined in the *Nomenclature* Section at the end of the paper. The right-hand side of Eq. 1 represents inflow and outflow of free and bound drug. The left-hand side gives a complete accounting for the accumulation of (*a*) free drug in actual tissue and equilibrium blood in the total tissue [as defined by Mapleson (8)]; (*b*) bound drug in the equilibrium blood; and (*c*) bound drug in the actual tissue.

Now with the assumption of linear binding and using effective protein fractions to account for the different levels of binding (see *References 3, 4*),

$$x_p = BC_p,\ x_{MB} = BC_M,\ x_{MT} = BC_M \quad \text{(Eq. 2)}$$

Eq. (1) becomes

$$\{[f_B + B(1 - f_B)]V_{MB} + [f_{MT} + B(1 - f_{MT})]V_{MT}\} \frac{dC_M}{dt} = Q_M[f_B + B(1 - f_B)](C_p - C_M) \quad \text{(Eq. 3)}$$

To simplify the equations, define

$$\phi_B \equiv [f_B + B(1 - f_B)],\ \phi_{MT} \equiv [f_{MT} + B(1 - f_{MT})]$$

With a similar treatment for the other compartments, the full set of equations becomes (refer to Fig. 2):

$$\phi_B V_p \frac{dC_p}{dt} = Mg(t) + Q_L \phi_B C_L + Q_K \phi_B C_K + Q_M \phi_B C_M - Q_p \phi_B C_p \quad \text{(Eq. 4)}$$

$$(\phi_B V_{MB} + \phi_{MT} V_{MT}) \frac{dC_M}{dt} = Q_M \phi_B (C_p - C_M) \quad \text{(Eq. 5)}$$

$$(\phi_B V_{KB} + \phi_{KT} V_{KT}) \frac{dC_K}{dt} = Q_K \phi_B (C_p - C_K) - k_K C_K \quad \text{(Eq. 6)}$$

$$(\phi_B V_{LB} + \phi_{LT} V_{LT}) \frac{dC_L}{dt} = (Q_L - Q_G)\phi_B C_p + Q_G \phi_B C_G - Q_L \phi_B C_L - k_L C_L U(t - D_L) \quad \text{(Eq. 7)}$$

$$(\phi_B V_{GB} + \phi_{GT} V_{GT}) \frac{dC_G}{dt} = Q_G \phi_B (C_p - C_G) + k_0 U(t - D_L) \quad \text{(Eq. 8)}$$

$$Q_p = Q_M + Q_K + (Q_L - Q_G) + Q_G \quad \text{(Eq. 9)}$$

Also, a balance on the gut lumen, assuming again a lumped compartment gives,

$$\frac{dM_{GL}}{dt} = k_L C_L U(t - D_L) - k_0 U(t - D_L) - k_F M_{GL} U(t - D_F) \quad \text{(Eq. 10)}$$

The bile excretion term in Eq. 7 contains a time delay term, $U(t - D_L)$, to approximate the bile formation and holding time. A continuous *s*-shaped function would be more realistic but would introduce additional mathematical complexity not considered important to this preliminary work. The same time delay appears in the zero-order gut absorption term in Eq. 8 since absorption cannot occur before the bile appears from the liver. These time delays appear also in Eq. 10 for the gut lumen with an additional time delay in the feces removal term, $U(t - D_F)$, representing the travel time down the small intestine.

As discussed in detail in Bischoff and Dedrick (9), with linear binding the above equations can be written in terms of total (free and bound) concentration in a simple form, with each parameter maintaining a well-defined physiological meaning. The concentrations actually measured in the laboratory were total wet tissue values, indicated by:

$$C_p' = \phi_B C_p \qquad \text{(Eq. 11)}$$

$$C_M' = \frac{\phi_B V_{MB} + \phi_{MT} V_{MT}}{V_{MB} + V_{MT}} C_M \qquad \text{(Eq. 12)}$$

$$C_K' = \frac{\phi_B V_{KB} + \phi_{KT} V_{KT}}{V_{KB} + V_{KT}} C_K \qquad \text{(Eq. 13)}$$

$$C_L' = \frac{\phi_B V_{LB} + \phi_{LT} V_{LT}}{V_{LB} + V_{LT}} C_L \qquad \text{(Eq. 14)}$$

$$C_G' = \frac{\phi_B V_{GB} + \phi_{GT} V_{GT}}{V_{GB} + V_{GT}} C_G \qquad \text{(Eq. 15)}$$

The basis of these equations can be stated in words:

$$C_M' = \frac{\left\{\left[\begin{array}{c}\text{amount in}\\ \text{equilibrium blood}\end{array}\right] + \left[\begin{array}{c}\text{amount in}\\ \text{actual tissue}\end{array}\right]\right\}}{\text{(total volume of equilibrium blood and tissue)}}$$

$$= \left\{\left[\begin{array}{l}\text{(free + bound concentration in equilibrium}\\ \text{blood)(volume of equilibrium blood)}\end{array}\right]\right.$$

$$\left. + \left[\begin{array}{l}\text{(free + bound concentration in actual}\\ \text{tissue)(volume of actual tissue)}\end{array}\right]\right\} \Big/ \text{(total volume)}$$

$$= \frac{[f_B + B(1 - f_B)]C_M V_{MB} + [f_{MT} + B(1 - f_{MT})]C_M V_{MT}}{V_{MB} + V_{MT}}$$

This then leads to Eq. 12. Similar reasoning was used for the other tissues.

The equilibrium (tissue/plasma) ratios are indicated by:

$$R_M \equiv \left(\frac{C_M'}{C_p'}\right)_{eq.} = \frac{\phi_B V_{MB} + \phi_{MT} V_{MT}}{\phi_B (V_{MB} + V_{MT})} \qquad \text{(Eq. 16)}$$

$$R_K \equiv \left(\frac{C_K'}{C_p'}\right)_{eq.} = \frac{\phi_B V_{KB} + \phi_{KT} V_{KT}}{\phi_B (V_{KB} + V_{KT})} \qquad \text{(Eq. 17)}$$

and similarly for R_G and R_I. These distribution ratios permit the relation between total and free concentrations to be written in a simpler form:

$$C_M' = \phi_B R_M C_M \qquad \text{(Eq. 18)}$$

and similarly for the others. If these relations are substituted into the mass balances, Eqs. 4–10, the final form is:

$$V_p \frac{dC_p'}{dt} = Mg(t) + Q_L \frac{C_L'}{R_L} + Q_K \frac{C_K'}{R_K} + Q_M \frac{C_M'}{R_M} - Q_p C_p' \qquad \text{(Eq. 19)}$$

$$(V_{MB} + V_{MT}) \frac{dC_M'}{dt} = Q_M \left(C_p' - \frac{C_M'}{R_M}\right) \qquad \text{(Eq. 20)}$$

$$(V_{KB} + V_{KT}) \frac{dC_K'}{dt} = Q_K \left(C_p' - \frac{C_K'}{R_K}\right) - \frac{k_K}{\phi_B R_K} C_K' \qquad \text{(Eq. 21)}$$

$$(V_{GB} + V_{GT}) \frac{dC_G'}{dt} = Q_G \left(C_p' - \frac{C_G'}{R_G}\right) + k_0 U(t - D_L) \qquad \text{(Eq. 22)}$$

$$(V_{LB} + V_{LT}) \frac{dC_L'}{dt} = (Q_L - Q_G)\left(C_p' - \frac{C_L'}{R_L}\right) + Q_G \left(\frac{C_G'}{R_G} - \frac{C_L'}{R_L}\right) - \left(\frac{k_L}{\phi_B R_L}\right) C_L' U(t - D_L) \qquad \text{(Eq. 23)}$$

$$\left(\frac{dM_{GL}}{dt}\right) = -k_0 U(t - D_L) - k_F M_{GL} U(t - D_F) + \left(\frac{k_L}{\phi_B R_L}\right) C_L' U(t - D_L) \qquad \text{(Eq. 24)}$$

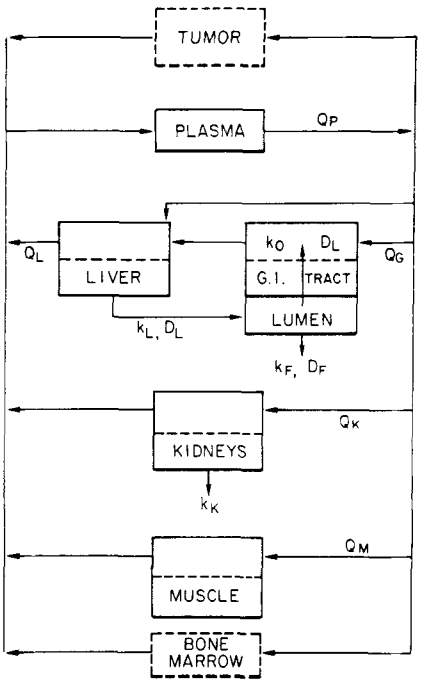

Figure 2—*Compartmental model for MTX distribution. The bone marrow and a hypothetical tumor are indicated because these are regions of interest even though they would normally exert little influence on systemic drug distribution kinetics.*

It should be again emphasized that all of the volume, flow, and other parameters in these equations have well defined physiological meanings and are not derived by "curve fitting" to an arbitrary set of functions.

This set of simultaneous linear differential equations could be solved analytically albeit with considerable algebraic complexity. Figure 1 shows that several of the regions are characterized by similarly shaped curves with different levels. These different levels can be accounted for by the distribution ratios, and thus it would appear that some of the equations could be combined by assuming that these tissues are essentially in physical distribution equilibrium. In particular, this is true of the highly perfused viscera, except for the liver which is complicated by the bile formation at short times. Similar behavior is found for other drugs—see Bischoff and Dedrick (9). The poorly perfused muscle tissue does not exactly follow the same pattern, particularly at short times, but since the muscle tissue is not of primary importance and also does not contain a large fraction of the drug, the simplifying equilibrium assumption will also be used. Using Eqs. 16–17, this means

$$C_M' = R_M C_p' \qquad \text{(Eq. 25a)}$$

$$C_K' = R_K C_p' \qquad \text{(Eq. 25b)}$$

$$C_G' = R_G C_p' \qquad \text{(Eq. 25c)}$$

and Eqs. 19–23 condense to:

$$V_p' \frac{dC_p'}{dt} = Q_L \left(\frac{C_L'}{R_L} - C_p'\right) - k_K' Cp' + Mg(t) \qquad \text{(Eq. 26a)}$$

where

$$V_p' \equiv V_p + R_M V_M + R_K V_K + R_G V_G \qquad \text{(Eq. 26b)}$$

and

$$V_L \left(\frac{dC_L'}{dt}\right) = Q_L \left(C_p' - \frac{C_L'}{R_L}\right) - k_L' \frac{C_L'}{R_L} \times U(t - D_L) + k_0 U(t - D_L) \qquad \text{(Eq. 27)}$$

Figure 3 is a diagram of the simplified model. A slight modification of the transport network, shifting the gut absorption term from the main body compartment to the liver compartment, is made to more closely correspond to actual anatomy.

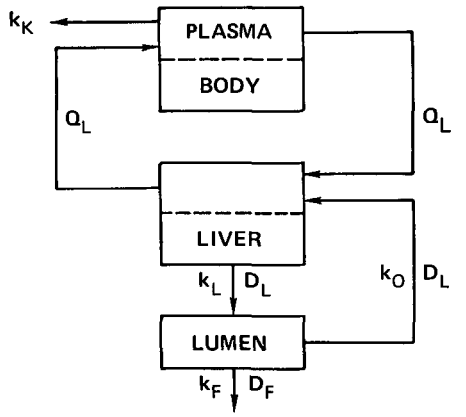

Figure 3—*Two-compartment model plus gut lumen.*

These equations can be readily solved for all times, but for these initial studies, further simplification is useful. Figure 1 shows that for all but short times, the liver behavior is similar to that of plasma and other tissues. Thus, for the longer-time regime:

$$C_L' = R_L C_p' \qquad \text{(Eq. 28)}$$

Eqs. 26, 27, and 24 condense to

$$V_p''\left(\frac{dC_p'}{dt}\right) = Mg(t) - k_K' C_p' - k_L' C_p' U(t - D_L) + k_0 U(t - D_L) \qquad \text{(Eq. 29}a\text{)}$$

where

$$V_p'' \equiv V_p' + R_L V_L \qquad \text{(Eq. 29}b\text{)}$$

$$\left(\frac{dM_{GL}}{dt}\right) = -k_0 U(t - D_L) - k_F M_{GL} U(t - D_F) + k_L' C_p' U(t - D_L) \qquad \text{(Eq. 30)}$$

Figure 4 is a diagram of this model.

PARAMETER VALUES

The parameter values for the models are summarized in Table I. Those directly measured are averages from several mice, and those from correlations are adjusted to the mean-size standard mouse of 22 g.

EQUATION SOLUTIONS AND RESULTS

The various model equations are solved for sequential time steps. For $0 \leq t_1 \leq D_L$, the solutions to Eqs. 26 and 27 with an impulse i.v. injection, $g(t) = \delta(t)$, and with zero initial conditions, $C_{p_1}'(0) = 0$, $C_{L_1}'(0) = 0$, $M_{GL_1}(0) = 0$, are:

$$\frac{C_{p_1}' V_p'}{M} = \frac{\left(r_2 + \frac{Q_L}{R_L V_L}\right) e^{r_2 t} - \left(r_1 + \frac{Q_L}{R_L V_L}\right) e^{r_1 t}}{r_2 - r_1} \qquad \text{(Eq. 31)}$$

$$\frac{C_{L_1}' V_p'}{M} = \frac{Q_L}{R_L V_L} \frac{e^{r_2 t} - e^{r_1 t}}{r_2 - r_1} \qquad \text{(Eq. 32)}$$

$$M_{GL_1} \equiv 0 \qquad \text{(Eq. 33)}$$

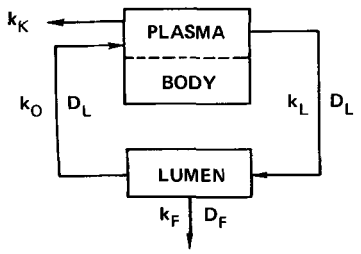

Figure 4—*Single-compartment model plus gut lumen.*

Table I—Model Parameters for 22-g. Mouse

Parameter	Value
V_p	1 ml.
V_G, Gut wall and contents	1.5 g.
V_K	0.34 g.
V_M	~10 g.
V_L	1.3 g.
R_G, Intestine tissue	0.15, Estimate
R_K	3
R_M	0.15
R_L	10
R_{bile}	300
k_K'	0.26 ml./min.[a]
k_L'	0.75–1.1 ml./min.[b]
k_0 For 3 mg./kg.	0.39 mcg./min. = 0.64%/min.
k_F, Mean residence time^{-1}	$\frac{1}{120}-\frac{1}{180}$ min.$^{-1}$ = 7.5×10^{-3} min.$^{-1}$
D_L	~2.5–5 min.
D_F	~120–180 min.

[a] Inulin clearance reported by Selkurt (13) per gram of rat kidney: (0.75 ml./min. g. kidney) (0.34 g. kidney) = 0.26 ml./min. [b] Biliary clearance bounds estimate by: (*a*) maximum clearance = hepatic plasma, flow rate = (1.4 ml./min. ml. liver)* (1.3 g. liver) × (0.6 ml. plasma/ml. blood) = 1.1 ml./min.; (*b*) minimum clearance = (bile flow rate)(MTX concentration ratio) = (2.5 μl./min.)(300) = 0.75 ml./min. * Bradley, *Reference 13.*

where

$$r_{(\frac{1}{2})} = -\tfrac{1}{2}\left[\frac{k_M'}{V_p'} + \frac{Q_L}{V_p'}\left(1 + \frac{V_p'}{R_L V_L}\right)\right] \pm R \qquad \text{(Eq. 34}a\text{)}$$

$$R \equiv \sqrt{\tfrac{1}{4}\left[\frac{k_K'}{V_p'} + \frac{Q_L}{V_p'}\left(1 + \frac{V_p'}{R_L V_L}\right)\right]^2 - \frac{Q_L k_K'}{V_p' R_L V_L}} \qquad \text{(Eq. 34}b\text{)}$$

With the parameter values for a dose of 3 mg./kg.,

$$C_{p_1}' = 4.57e^{-0.014 t_1} + 26.6e^{-0.496 t_1} \qquad \text{(Eq. 35)}$$

$$C_{L_1}' = 54.9(e^{-0.014 t_1} - e^{-0.496 t_1}) \qquad \text{(Eq. 36)}$$

For the next time period, $D_L \leq t_2 \leq D_F$ and with initial conditions $C_{p_2}'(0) = C_{p_1}'(D_L)$, $C_{L_2}'(0) = C_{L_1}'(D_L)$, $M_{GL}(0) \simeq 0$ and $g(t) \equiv 0$ the solution to Eqs. 29 and 30 are:

$$C_{p_2}' = \frac{k_0}{\sigma} + \left(C_{p_1}'(D_L) - \frac{k_0}{\sigma}\right) e^{-(\sigma/V_p'')t_2} \qquad \text{(Eq. 37)}$$

where

$$\sigma = k_K' + k_L'$$

$$M_{GL_2} = -\frac{k_0 k_K'}{\sigma} t_2 + \frac{K_L' V_p''}{\sigma}\left(C_{p_1}'(D_L) - \frac{k_0}{\sigma}\right)(1 - e^{-(\sigma/V_p'')t_2}) \qquad \text{(Eq. 38)}$$

Again with the parameters for 3 mg./kg.

$$C_{p_2}' = 0.508 + 6.0e^{-0.0777 t_2} \qquad \text{(Eq. 39)}$$

and

$$\left(\frac{M_{GL}}{V_G}\right) = -0.088 t_2 + 51.3(1 - e^{-0.0777 t_2}) \qquad \text{(Eq. 40)}$$

Finally, for long times, $t_3 > D_F$, the data indicate in Fig. 5 that the plasma and tissue concentrations are essentially constant. These data are not highly accurate, however, since, as can be seen in the plots, they represent less than 1% of the dose. Thus the radioactivity measured could result from substances other than MTX, from irreversible binding, or other small deviations. Nevertheless, in this regime

$$C_{p_3}' \simeq \frac{k_0}{\sigma} \qquad \text{(Eq. 41}$$

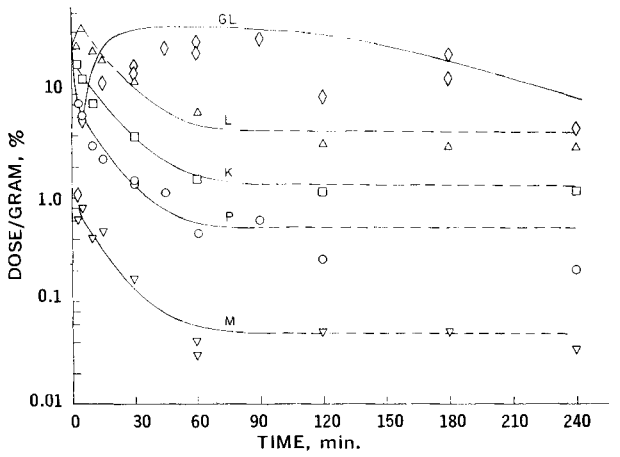

Figure 5—*Comparison between curves predicted by equations and observed data.*

and

$$M_{GL_3} = \left(M_{GL_2}(D_F) + \frac{k_0 k_K'}{\sigma k_F}\right) e^{-k_F t_3} - \frac{k_0 k_K'}{\sigma k_F} \quad \text{(Eq. 42)}$$

For 3 mg./kg.

$$C_{p_3}' = 0.508 \quad \text{(Eq. 43)}$$

$$\left(\frac{M_{GL_3}}{V_G}\right) = 52e^{-0.0075t_3} - 12 \quad \text{(Eq. 44)}$$

Comparison of the *a priori* predicted results with the data of Fig. 1 is shown in Fig. 5. Eqs. 35 and 36 are used up to $D_L \sim 5$ min., Eqs. 39 and 40 to $D_F \sim$ 120–180 min., and Eqs. 43 and 44 for the remaining time. On the whole, excellent agreement is obtained, but several comments are in order. For very short times, Eqs. 26 and 27 depend upon essentially instantaneous equilibration between all parts of the body except for the liver. This results in the nearly vertical line from 100% dose/1 ml. plasma to 31% dose/3.2 ml. body, which is $C_{p_1}'(0)$.

The major discrepancy is the gut lumen predictions for $t < 60$ min., where the predicted value is too high. Probably the main reason for this is the assumption of pure transport time delays which implies abrupt infusion of concentrated bile into the gut lumen at $t = D_L$. As more data are obtained, a better model for biliary clearance should be possible. Another modification would be to use a plug flow model of the small intestine rather than the simple lumped compartment. This approach is now under consideration, and the authors also have some data on drug passage through the intestines. The liver curve between 5 and 30 min. does not completely parallel the plasma curve, and so Eq. 28 is not exactly correct early in the second time region. The full two-compartment equations will be used eventually.

FUTURE WORK

Based on these encouraging initial results, work is in progress to extend and verify the model in several directions. One is to consider other dose levels. Because of the linear nature of the mathematical model, the relative concentrations should remain the same except for possible changes in absorption or excretion mechanisms. For smaller doses, the saturated zero-order gut absorption should become first order if a simple Michaelis-Menten form is followed. Some work by Burgen and Goldberg (10) using direct perfusion methods indicate that this happens for folic acid, which is close in chemical structure to MTX. Both their data and results of Henderson *et al.* (6) suggest that such behavior might occur at dose levels of ~0.1 mg./kg., which is much smaller than the 3 mg./kg. used here. This phenomenon merits careful investigation. Evidence by Guarino and Schanker (11) suggests that the bile excretion mechanism becomes saturated at high doses. Additional information in this regard is required. Data by Borsa *et al.* (12) indicate that this may be true with MTX in mice.

For some of these future studies, the simple form of the differential equations will not suffice and analytical solutions may no longer be possible. The two-compartment model for short times will be utilized using numerical computation techniques to describe more accurately the very important action of the liver and biliary excretion. With more data concerning the latter process, the abrupt time-delay forms will probably also be modified to use a continuous sigmoid rather than a step function—this could also be readily handled with the computer solutions.

Finally, the fundamental issues of scale-up will be emphasized. Some data on rats are now available, and an attempt will also be made to directly apply the model to these data as well as to published human clinical data.

NOMENCLATURE

B = binding constant, dimensionless
C = free concentration, mcg./ml.
C' = total concentration, mcg./ml., Eqs. 11–15
D = delay time, min.
f = fraction water, dimensionless
$g(t)$ = injection function, min.$^{-1}$
k = clearance, ml./min.
k' = clearance based on total concentration in plasma, ml./min.
k_0 = gut absorption rate, mcg./min.
M = amount of drug, mcg.
Q = flow rate, ml./min.
$r_{(\frac{1}{2})}$ = defined in Eqs. 34*a* and *b*
R = equilibrium tissue/plasma ratio, dimensionless
t = time, min.
U = time delay function, dimensionless
V = volume of compartment, ml.
V' = defined by Eq. 26*b*, ml.
V'' = defined by Eq. 29*b*, ml.
x = bound concentration, mcg./ml.
ϕ = defined below Eq. 3, dimensionless
σ = defined below Eq. 37, ml./min. $= k_K' + k_L'$

SUBSCRIPTS

B = blood
F = feces
G = gut
GB = gut equilibrium blood
GL = gut lumen
GT = gut equilibrium tissue
K = kidney
KB = kidney equilibrium blood
KT = kidney equilibrium tissue
L = liver
LB = liver equilibrium blood
LT = liver equilibrium tissue
M = muscle
MB = muscle equilibrium blood
MT = muscle equilibrium tissue
P = plasma
1, 2, 3 = three time periods of integration: $0 \leq t_1 \leq D_L$; $D_L \leq t_2 \leq D_F$; $t_3 > D_F$

REFERENCES

(1) K. B. Bischoff and R. G. Brown, *Chem. Eng. Progr. Symp. Ser. 66*, **62**, 32(1966).

(2) K. B. Bischoff, in "Chemical Engineering in Medicine and Biology," D. Hershey, Ed., Plenum, New York, N. Y., 1967, p. 417.

(3) R. L. Dedrick and K. B. Bischoff, *Chem. Eng. Progr. Symp. Ser. 84*, **64**, 32(1968).

(4) K. B. Bischoff and R. L. Dedrick, *J. Pharm. Sci.*, **57**, 1346 (1968).

(5) E. S. Henderson, R. H. Adamson, C. Denham, and V. T. Oliverio, *Cancer Res.*, **25**, 1008(1965).

(6) E. S. Henderson, R. H. Adamson, and V. T. Oliverio, *ibid.*, **25**, 1018(1965).

(7) E. E. Selkurt, in "Handbook of Physiology," Section 2, Circulation, vol. 2, Am. Physiol. Soc., 1963, p. 1483.

(8) W. W. Mapleson, *J. Appl. Physiol.*, **18**, 197(1963).
(9) K. B. Bischoff and R. L. Dedrick, unpublished data, 1969.
(10) A. S. V. Burgen and N. J. Goldberg, *Brit. J. Pharmacol.*, **19**, 313(1962).
(11) A. M. Guarino and L. S. Schanker, *J. Pharmacol. Exptl. Therap.*, **164**, 387(1968).
(12) J. Borsa, A. F. Whitmore, F. A. Valeriote, D. Collins, and W. R. Bruce, *J. Natl. Cancer Inst.*, **42**, 235(1969).
(13) S. E. Bradley, in "Handbook of Physiology," Section 2, 1963, Circulation, vol. 2, *Am. Physiol. Soc.*, p. 1405.

ACKNOWLEDGMENTS AND ADDRESSES

Received July 14, 1969, from the *National Institutes of Health, Public Health Service, U. S. Department of Health, Education, and Welfare, Bethesda, MD 20014*

Accepted for publication September 10, 1969.

This investigation was supported in part by a National Institutes of Health fellowship 1-F3-GM39 700-01 from the National Institute of General Medical Sciences.

* Permanent address: Department of Chemical Engineering, University of Maryland, College Park, Md.

Intestinal Drug Absorption and Metabolism I: Comparison of Methods and Models to Study Physiological Factors of *In Vitro* and *In Vivo* Intestinal Absorption

WILLIAM H. BARR* and SIDNEY RIEGELMAN†

Abstract □ Two experimental methods for use in kinetic studies on a compartment model for intestinal metabolism and absorption were evaluated. The *in vitro* cannulated everted intestinal sac and the *in vivo* intestinal loop with complete mesenteric venous collection were compared in the same region of rabbit intestine. These experimental methods were used to study the effects of metabolism, tissue accumulation, and blood flow on the transport of salicylamide across the basal barrier and provide experimental evidence to support the cell compartment model. At lower initial mucosal concentration (10^{-3} *M*), over 60% of the drug appearing in mesenteric blood is conjugated with glucuronic acid. At higher initial mucosal fluid concentrations, glucuronide conjugation appears to be capacity limited and the disappearance from the lumen-curve shows a distinct distributive phase characteristic of a cell compartment model. The rate of transport of free drug across the basal barrier is blood flow rate-limited while the transport of glucuronide is essentially independent of blood flow. Appearance of free salicylamide into mesenteric blood, *in vivo*, shows a lag time of 4 min. compared to a lag time of about 10 min. for the appearance of free drug into serosal fluid *in vitro*. The steady state rate of appearance of free drug into the plasma (*in vivo*) is five to ten times greater than the rate of appearance of free drug into the serosal fluid (*in vitro*) at similar mucosal concentrations. The *in vivo* intestinal loop with complete venous collection was found to have many advantages in studying physiological factors of intestinal drug absorption.

Keyphrases □ Drug absorption—intestinal □ Everted intestine—drug absorption, *in vitro* □ Intestinal loop, cannulated—drug absorption, *in vivo* □ Salicylamide—absorption, accumulation, metabolism □ Glucuronic acid-salicylamide conjugation—concentration effect □ Fluorometry—analysis

From the standpoint of a drug administered orally to produce a systemic effect, intestinal absorption can be considered as the amount of unchanged drug absorbed from the intestinal lumen which appears in the portal circulation or intestinal lymph. Using this definition, the amount of drug disappearing from the lumen contents is sufficient to characterize the absorption process only if it reflects the rate of appearance of unaltered drug in the blood. If one accepts the above definition, then it becomes quite important to evaluate critically the widely used (1) practice of assessing absorption by monitoring only the rate of disappearance of drug from the lumen. The condition that the rate of disappearance of free (unaltered) drug from the lumen contents is identical to the rate of appearance of free drug in the mesenteric blood is implicit in the classical lipoid barrier model of intestinal absorption which assumes that the intestinal tissue is a single barrier which does not contribute to the material balance of the system.[1] When accumulation or metabolism of drug occurs in the intestinal tissue, these rates may not be identical and a tissue compartment model for absorption is considered here as a more appropriate model to describe the entire absorption sequence.

The studies described in this report were designed to compare *in vivo* and *in vitro* experimental methods and mathematical models that might be useful in studying the effect of physiological factors, such as accumulation and metabolism of drug in the intestinal tissue and intestinal blood flow, on the appearance of free drug into mesenteric blood.

The general multiple barrier tissue compartment model that will be used to describe these physiological variables in *in vivo* and *in vitro* preparations is shown in Fig. 1. This catenary three-compartment model assumes that the intestinal tissue can be described as a homogeneous compartment, which is separated from the lumen compartment by an apical barrier (α) and from the terminal blood or serosal fluid compartment by a

[1] In compartment theory, a barrier may be defined as that rate-limiting step between two compartments which distinguishes these compartments by the fact that the rate of distribution within each compartment is sufficiently rapid, compared to the rate of transport across the barrier, that each compartment may be described by a separate volume of distribution. The barrier is considered to be only a rate-limiting step of negligible volume which does not contribute to or alter the material balance of the system. See, for example, the discussion on the concept of a barrier by Riggs (*Reference 32*, p. 188) and the concept of a compartment being represented as a volume by Resigno and Segre (*Reference 31*, p. 16).